HEAD POSE ESTIMATION IN FACE RECOGNITION ACROSS POSE SCENARIOS

M. Saquib Sarfraz and Olaf Hellwich

Computer vision and Remote Sensing, Berlin university of Technology
Sekr. FR-3-1, Franklinstr. 28/29, D-10587, Berlin, Germany.
{saquib;hellwich}@fpk.tu-berlin.de

Keywords: Pose estimation, facial pose, face recognition, local energy models, shape description, local features, head pose classification.

Abstract: We present a robust front-end pose classification/estimation procedure to be used in face recognition scenarios. A novel discriminative feature description that encodes underlying shape well and is insensitive to illumination and other common variations in facial appearance, such as skin colour etc., is proposed. Using such features we generate a pose similarity feature space (PSFS) that turns the multi-class problem into two-class by using inter-pose and intra-pose similarities. A new classification procedure is laid down which models this feature space and copes well with discriminating between nearest poses. For a test image it outputs a measure of confidence or so called posterior probability for all poses without explicitly estimating underlying densities. The pose estimation system is evaluated using CMU Pose, Illumination and Expression (PIE) database.

1 INTRODUCTION

Out of plane rotation of face has long been one of the bottlenecks in the face recognition area. A face recognition system should be able to handle variations in face images due to pose, illumination and other changes.

Recent research direction, in handling variations due to pose, has been to first estimate the pose of the test input face and then transform it to an already learned reference pose (Lee and Kim, 2006). Pose estimation/classification is thus a very useful front-end processing tool for multi-view human face analysis.

In 2D context, methods for face pose estimation are either based on landmark feature detection (Zhao and Gao, 2006), appearance based subspace methods, treating the whole face as one feature vector in some feature subspace(Gong, 1996), or a combination of both (Grundig and Hellwich, 2004). The former uses certain localized landmarks points on the image and tries to estimate the pose information by modelling the displacement of these points across multiple poses. This, however, is very sensitive to accurate localization of landmarks and also assumes that the ratios of these points do not change significantly

under different facial expressions. Sub-space methods, on the other hand, although avoids these problems of landmarks localization and modelling, but it assumes that inter-pose variations are always larger than intra-pose variations. This, generally, is not true since different subjects across same pose may have large appearance variations due to e.g. glasses, expressions, illumination and skin colour.

In this paper, we propose a method which overcomes these problems and is robust against the aforementioned appearance variations across same pose. We introduce a novel feature descriptor; Local Energy based Shape Histogram (LESH), which is based on local energy model of feature perception. As stated in (kovesi, 2000), the local energy response of an image is obtained by using Gabor filtering, which gives relatively stable response in terms of high energy on edges corners etc. On facial images this will have high energy response along landmark facial features such as eyes, nose and lips.

The proposed feature description models this energy response in terms of local filter orientations into a compact spatial histogram. These features have good discriminative ability among large pose variations. However, in order to discriminate between adjacent poses and to cater in-pose variations, due to other factors like glasses etc, we

need to learn these variations in a training phase. For this, we propose an efficient learning procedure which turns the multi-class problem into a two-class one by modelling a pose similarity feature space (PSFS) obtained from extra-pose (different pose) and intra-pose (same pose) similarities in the training phase. For a test image it outputs a measure of confidence or probability for all poses without explicitly estimating underlying densities. Our system is evaluated on CMU-PIE face database (Sim and Baker, 2002).

In section 2 we explain our approach for the proposed feature extraction and description. Section 3 describes the pose estimation and classification procedure in detail. With experimental results in section 4, we conclude in section 5 with a brief discussion.

2 FEATURE EXTRACTION

Multi-resolution Gabor based features are widely used and proven very useful in face recognition. Recently, (Baochang *et all*, 2007) has shown that local Gabor phase patterns can provide a very informative description and are quite useful in order to model the orientation of the head (Bingpeng *et all*, 2006). Another body of work exists which uses this phase information to compute the local energy content of the underlying signal, for detecting interest points such as corners, edges, valleys contours etc.

2.1 Local Energy Model

The local energy model developed by (Morrone and Owens, 1987) postulates that features are perceived at points in an image where the local frequency components are maximally in phase.

$$E(x) = \max_{\overline{\varphi}(x) \in [0, 2\pi]} \frac{\sum_n A_n \cos(\varphi_n(x) - \overline{\varphi}(x))}{\sum_n A_n} \quad (1)$$

Where A_n and φ_n are the magnitude and phase of the nth fourier component. This frequency information must be obtained in a way such that underlying phase information is preserved. For this linear phase filters must be used in symmetric anti symmetric pair. This is achieved by convolving the image with a bank of Gabor wavelets kernels tuned to 5 spatial frequencies and 8 orientations. At each image location, for each scale and orientation, it produces a complex value comprising the output of even

symmetric and odd symmetric filter, which gives the associated magnitude and phase of that pixel.

$$G_{u,v}(e_n, o_n) = I(x, y) * \psi_{u,v}(z) \quad (2)$$

Where $\psi_{u,v}$ is the bank of Gabor kernel and u,v is the scale and orientation.

Originally (Robbins and Owen, 1997) has proposed to use cosine of the deviation of each phase component from the mean phase as a measure of the symmetry of phase, however, this measure results in poor localization and is sensitive to noise. (Kovesi, 2000) extended this framework and developed a modified measure, as given in equation 3, consisting of sine of the phase deviation, including a proper weighing of the frequency spread W and also a noise cancellation factor T.

$$(3)$$

$$E = \frac{\sum_n W(x) \lfloor A_n(x)(\cos(\varphi_n(x) - \overline{\varphi}(x)) - |\sin(\varphi_n(x) - \overline{\varphi}(x))|) - T \rfloor}{\sum_n A_n(x) + \varepsilon}$$

The normalization by summation of all component amplitudes makes it independent of the overall magnitude of the signal, making it invariant to illumination variations in images. For details of this measure see (kovesi, 2000).

2.2 Proposed Feature Description

The local energy analysis in the preceding section is intended to detect interest points in images with a high reliability in presence of illumination and noise. Hence, to detect these i2D structures (Kovesi, 2003) proceeds by constructing principal moments of this normalized energy measure, also termed as phase congruency. In contrast to this, we rather use this raw energy information and attempt to encode the underlying shape. This is done in a way that makes it invariant to scale variations but not to rotation since rotation is precisely what we are trying to model.

2.2.1 LESH - Local Energy based Shape Histogram

Motivated by the fact that this local orientation energy response varies with respect to the underlying shape, in our case the rotation of head and since local energy signifies the underlying corners, edges or contours, we generate a local histogram accumulating the local energy along each filter orientation on different sub-regions of the
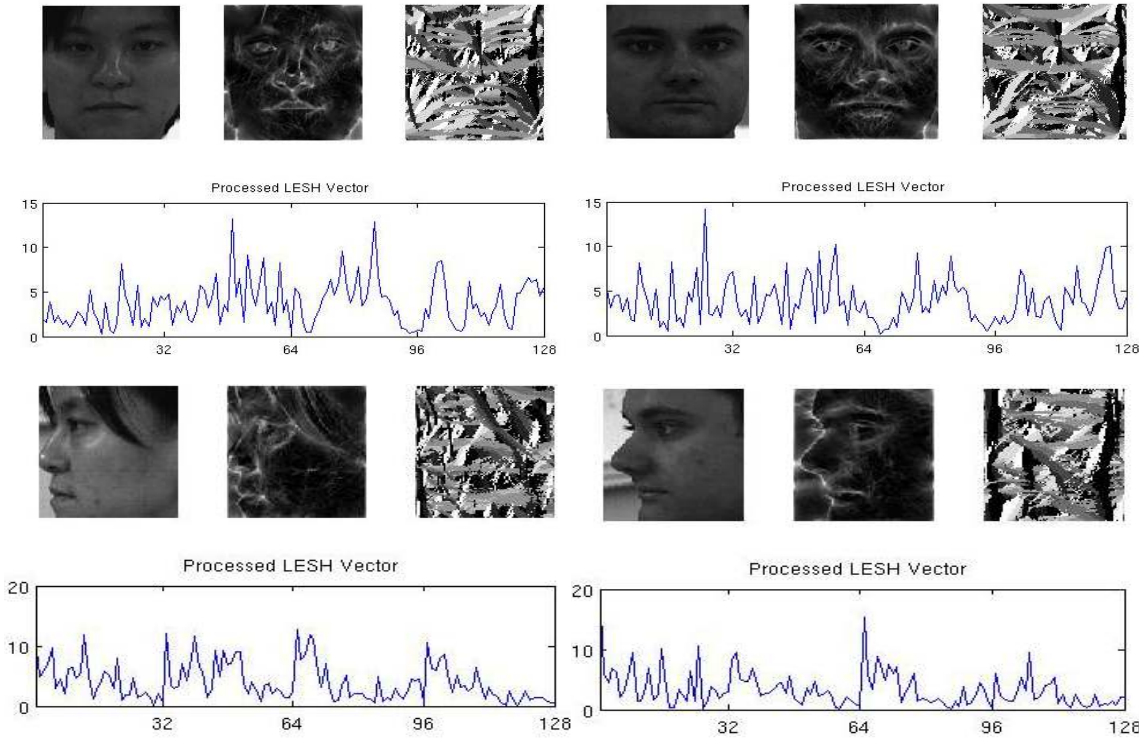
236

Figure 1: Two different subjects at frontal and left profile pose. Their associated energy and orientation maps and extracted LESH feature vectors.

image. The local histograms are extracted from different sub-regions of the image, and then concatenated together, to keep the spatial relationship between facial parts.

We proceed by obtaining an orientation label map where each pixel is assigned the label of the orientation at which it has largest energy across all scales.

The local histogram 'h' is extracted according to the following:

$$h_{r,b} = \sum w_r \times E \times \delta(L - b) \qquad (4)$$

Where subscript 'b' represents the current bin, 'L' is the orientation label map, 'E' is the local energy, as computed in equation 3, and 'w' is a Gaussian weighing function centred at region 'r'.

$$w_r = \frac{1}{\sqrt{2\pi\sigma}} e^{[(x-r_{xo})^2 + (y-r_{yo})^2]/\sigma^2} \qquad (5)$$

This weight is used to provide soft margins across bins by small weighted overlap among neighbouring sub-regions to overcome the problems induced due to scale variations. In our experiments, for a 32x32 region, σ is set to 20 in both directions.

As mentioned earlier, in order to keep the spatial relation between facial parts, we extract 8 bins local histogram corresponding to 8 filter orientations on 16 image partitions, which makes it a 128-dimentional feature vector.

Example feature extraction and associated energy and orientation maps on two different subjects in frontal and left profile pose, from CMU-PIE database, are shown in Figure 1.

Figure 1 provides an intuitive look at the notion of similarity across same pose among different subjects, in terms of extracted local energy and LESH features. This notional similarity is validated empirically in section 3 by computing similarities between extracted LESH features. Note how they are quite invariant to person specific appearance variations.

3 POSE ESTIMATION

The derived LESH features in the preceding section provide a strong foundation on which to base our pose estimation framework. These features are robust against slight misalignment and scale changes, but this comes with the cost of rather loose description of facial landmark positions. Although this does not affect while discriminating among large pose variations such as the one shown in figure

Figure 2: (along Rows) All 9 pose variations in CMU-PIE; pose 1(right profile) to pose 9 (left profile) views; (Along columns) 7 imaging conditions; illumination and expression variations.

1, but discriminating among nearest pose changes, by simply looking at similarity scores, is quite error prone. Also, other variations, such as glasses, expressions and to some extent illumination (shadows), hinder a direct matching of these features to decide on pose.

We therefore, learn these variations across same pose from a training procedure in a novel way. In particular, we lay down an effective classification procedure that attempts to model these in pose variations and performs quite well in discriminating among slight pose variations.

Before explaining our pose estimation framework, we introduce the facial database used in our experiments.

3.1 PIE Database

We used a subset of PIE database to evaluate our pose estimation algorithm. The portion of PIE database, we used, consists of 21 illumination differences of 68 subjects at 9 poses. Where 4 different illumination variations (out of 21) and 3 PIE expression variations per subject per pose are considered, see figure 2 for an example.

Following the PIE naming convention illumination variations correspond to flash 01, 04, 13 and 14, which captures well the extent of illumination variations present, and expression variations are neutral, smiling and blinking at frontal lighting. 15 subjects are used for training and rest of 53 subjects for testing, amounting to 3339(7x53x9) test examples.

In such scenarios one can expect that there will be a huge overlap between nearest poses in the derived feature space. We therefore introduce a new classification framework which overcomes this and models well the in-pose variations due to large illumination and expression changes.

3.2 Proposed Approach

For the reasons stated earlier, we solve the pose estimation as a classification problem from a machine learning point of view. Instead of directly modelling the extracted features and solve it as a multiclass problem, we rather use similarity scores of these features within same pose and among different poses. This implies construction of a new feature space based on these computed similarities. Such an approach has huge benefit in that it effectively turns a multiclass problem into a binary two-class one while still representing well all the in-pose variations. We model this new feature space.

3.2.1 Pose Similarity Feature Space

We transform the whole problem into a new feature space termed as pose similarity feature space (PSFS). This PSFS is derived by computing similarities between LESH features, coming from same pose examples and similarities between features from all the different pose examples.

As measure of similarity, we use modified K-L divergence which is numerically stable, symmetric and robust with respect to noise and size of histogram bins. It actually gives a measure of dissimilarity between two histograms. Thus low values means more similar. It is defined as

$$d(H, K) = \sum_r \eta_r \sum_i (h_{i,r} \log \frac{h_{i,r}}{m_{i,r}} + k_{i,r} \log \frac{k_{i,r}}{m_{i,r}}) \quad (6)$$

Where, subscript 'r' runs over total number of regions(partitions) and 'i' over number of bins in each corresponding local histogram h and k, see section 2.2.1, 'm' is the corresponding bin's mean and 'η_r' is used as a provision to weigh each region of the face while computing similarity scores. This could be used, for instance, in overcoming the problems due to expressions, by assigning a lower weight to regions that are mostly affected. In our experiments, for now, this η is set to 1.

For each example in our training set, we compute these similarities with the rest of the examples in the same pose on derived LESH features. Concatenating them, give rise to an intra pose 'IP' (same pose) similarity vector. Similarly computing these similarities for each example with all other examples in a different pose give rise to an extra pose 'EP' similarity vector. Thus each example is now represented in a PSFS as a function of its similarities by these IP or EP vectors.

Note however, the dimensionality of this PSFS is a direct function of the total number of examples per pose in the training set. Therefore to put upper limit on the dimensionality of this derived PSFS and also to generate many representative IP and EP vectors for a test face, as explained shortly, we partition our training sets into some disjoint subsets in such a way that each subset has same number of subjects in each pose. To understand it better, consider, for example, our training set comprising of 15 subjects, where each subject is in 7 different illumination and expression imaging conditions in each of the 9 poses, see figure 2. Therefore we have 15x7(105) examples per pose.

Deriving a PSFS directly means a 105 dimensional feature space, while partitioning it into some disjoint subsets, such as each subset has all the 15 subjects but in some different combination of the imaging condition, would yield a 15 dimensional features space while still representing all the variations we want to model.

3.2.2 Formal Description of our Approach

Formally, our approach is that we first partition the training set into 'k' disjoint subsets (all N training examples per pose per subset), the subsets are disjoint in terms of the 7 imaging conditions (chosen such as each subject is at a different imaging condition in that subset).

In each subset, we then compute for each example, its similarity to the rest of the examples in the same pose on derived LESH features. Thus for 'N' examples per pose, we compute 'N-1' similarities for each example, concatenating them, give rise to a 'N-1' dimensional intra-pose (IP) similarity feature vector for each of the N examples. Extra-pose (EP) vectors are obtained similarly by computing these similarities between each example in one pose with n-1 examples in a different pose by leaving the same subject each time.

Thus we will have $(N \times P \times K)$ IP samples and $k(N \sum_{i=1}^{P-1}(p - i))$ EP samples for training. Where 'N' is number of examples/pose and 'P' is total number of pose.

Although there will be a large number of EP samples as compared to IP in the derived PSFS but we note that, IP samples tend to have low values as compared to EP and form a compact cluster in some sub-space of the PSFS.

This is validated in Figure 3 which shows a 3-D scatter plot of IP and EP samples from one of the subset, by randomly choosing 3 features from IP and EP similarity vectors. Note that IP samples are depicted from all of the 9 poses while only those EP samples are depicted which are computed among large pose variations, such as between frontal and left/right profile view or between left and right profile view. The scatter plot is shown in logarithmic scale for better viewing.

Figure 3 provides an intuitive look at how the problem is easily separable when there are large pose variations, while EP samples coming from nearest pose examples can be seen as causing a marginal overlap with the IP class.

The training set is used as a gallery and thus for a test face, computing its similarity with all of the examples in each pose in each subset of the gallery produces many representative similarity vectors for that test image. Therefore there is a good chance that more of the similarity vectors, coming from where the pose of the test face and gallery are same, falls in
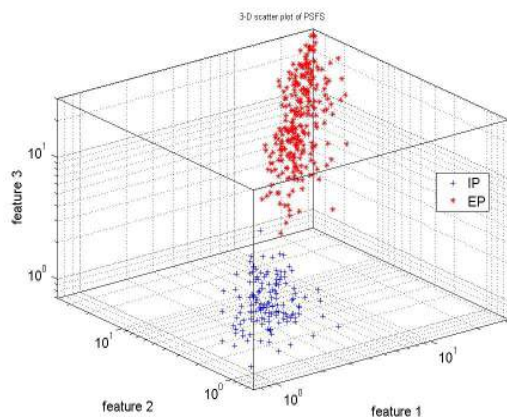
Figure 3: 3-D scatter plot of IP and EP vectors from one of the subset. IP samples are drawn by randomly choosing 3 features from IP vectors from all of the 9 poses, while EP samples are depicted only for large pose variations i.e. between frontal and left or right profile or between left and right profile view.

the IP class as compared to those which are coming from even slight pose variations.

To learn the structure of this PSFS, we therefore seek to separate the two classes. A simple AdaBoost classifier (Schapire and Singer, 1999), using nearest neighbour rule in each iteration, is trained in this feature space for this purpose. That provides a non-linear boundary between the two classes.

For a test image, k vectors are obtained for each pose by computing similarities from N-1 subjects in each pose in each training subset. All of these are classified to belong to either of the class. Final decision is then made by considering only those classified as IP, and assigning the label of the pose from which majority of these are coming. This probability for each pose is calculated simply by:

$$\gamma_p = \frac{\text{\# of vectors in pose p}}{\text{total \# of vectors}} \qquad ((7)$$

As stated earlier, the rational of making subsets of training set is now evident, as on one hand it limits the dimensionality of the feature space, while still representing well all the in-pose variations, and on the other hand it generates many representative vectors per pose for a test image, which provide us with a probability score and helps in overcoming the short comings of the classifier itself.

4 EXPERIMENTAL SETUP AND RESULTS

Each 640x480 pixel PIE image is converted to greyscale. A 128x128, closely cropped face part, which is adjusted to remove any tilt bias by using eye location is retained. We note that this is standard procedure and any state of the art face detector like (Kanade et all, 1998) can be used for this purpose.

As described in the preceding section, for the 15 training subjects we have (105)15x7 examples per pose. We partition them into 7 disjoint sets (each with 15 examples) for each pose, as described earlier.

This generates a 14 dimensional PSFS by computing all the IP and EP vectors using LESH features. AdaBoost is then trained on this PSFS.

For a test face, after extracting LESH feature, we compute similarities with 14 examples in each pose, for each training subset. This will generate one 14 dimensional similarity vector for each representative pose in each subset; therefore, we will have 7x1x9 (63) similarity vectors.

They are then classified as either IP or EP. Those which are assigned label as IP are then further used to compute probability scores, as described earlier, for each of the 9 poses.

Final pose estimate is based on by assigning the pose, which has highest score. This way we hope to overcome the problem of any misclassified nearest pose EP vectors.

Figure 4, on the next page, provides average estimation results for each pose. While Table 1 summarizes the classification results obtained on all the 371x9(3339) test examples in a confusion matrix.

The overall average estimation accuracy is 84.06% in terms of rank-1 rates and 96.62% for estimates within $\pm 22.5^\circ$ of accuracy.
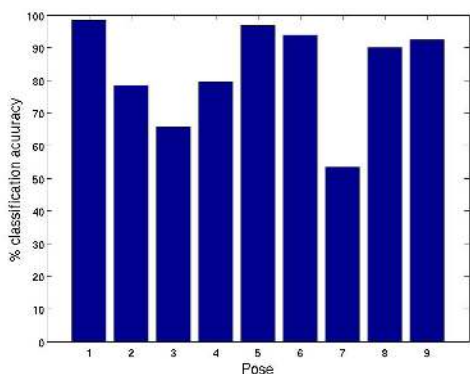
Figure 4: average classification scores for each pose.

Table 1: Confusion Matrix for all test examples.

| | | System Pose Estimates | | | | | | | | |
		1	2	3	4	5	6	7	8	9
T R U E P O S E	**1**	365	4	2	0	0	0	0	0	0
	2	47	291	24	6	2	0	0	1	0
	3	31	59	244	31	5	1	0	0	0
	4	0	0	21	295	39	2	0	0	0
	5	0	0	0	10	359	2	0	0	0
	6	0	0	0	0	17	348	5	1	0
	7	0	0	1	0	23	44	198	85	20
	8	0	0	0	0	0	4	11	334	22
	9	0	0	0	0	0	2	4	22	343

In confusion matrix, the rows entries are indexed by the true pose of the input images, while column entries are labelled by our classification procedure-determine pose. The entries on the diagonal indicate the number of correctly classified images at each pose. The sum of each row is 371 (an entry of 371 on the diagonal indicates perfect classification for that pose).

5   CONCLUSIONS & DISCUSSION

We can compare our results with few of the recent works (Yuan and casacent, 2005) and (Patnaik and casasent, 2005) which use same database and approximately the same setup, where former achieved 82.4% rank-1 and later achieved 84.11% rank-1 and 96.44% within $\pm22.5^{\circ}$, they however, pre- registered a test face to top 3 to 4 poses by using 3 landmark locations on the face and did not include expression variations.

Our system achieves best recognition scores on full profile views, the reason, perhaps, stems from the fact that a face at these views is most distinguishable in terms of pure shape. Since our system is build on a pure shape representation, these results provides an intuitive relation if one looks at the corresponding cropped faces at these poses, figure 2.

The performance of our method on registering a given face to the nearest pose (adjacent poses) is above 96%. It provides us with probabilities for each pose and that makes it very attractive from a practical stand point, since this can be used directly as our confidence in a given pose in the further face recognition stage.

On concluding remarks, we have presented a front-end pose estimation system which functions in presence of illumination and expression changes. A new feature description that encodes the underlying shape well is proposed, and an efficient classification procedure is suggested which turns the multi-class problem into a binary one and solves the problem of discriminating between nearest poses.

Based on this feature description, we introduced to generate a generic similarity feature space, that not only provides an effective way of dimensionality reduction but also provides us with many representative vectors for a given test feature vector.

This is used in generating probability scores for each pose without explicitly estimating the underlying densities, which is very useful in later face recognition across pose scenarios.

The system will be used for a subsequent transformation of a test face to a reference pose for face recognition.

We hope that the proposed feature description and the notion of modelling the similarity space will prove very useful in similar computer vision problems.

ACKNOWLEDGEMENTS

REFERENCES

Bingpeng M, Wenchao Z, Shiguang S, Xilin C, Wen G., 2006 "Robust Head Pose Estimation Using LGBP",ICPR, vol.2, pp512-515.

Baochang Z., Shiguang S., Xilin C., and Wen G., 2007 "Histogram of Gabor Phase Patterns (HGPP):A Novel Object Representation Approach for Face Recognition". IEEE Trans. on Image Processing, vol.16, No.1, pp57-68.

S. Gong, S. McKenna, and J. J. Collins. 1996 "An investigation into face pose distributions". In FG., pp 265.

Kovesi, P.D., 2000 "Phase congruency: A low-level image invariant" Psychological Research,64, pp136-148.

Kovesi,PD,2003,"phase congruency detects corners and edges", in proc. Australian pattern recognition society conference, pp 309-318.

Lee,H.S , Kim,D. 2006 "Generating frontal view face image for pose invariant face recognition", PR letters vol.27, No. 7, pp 747-754.

Morrone, M.C., Owens, R.A., 1987 "Feature detection from local energy". PR Letters(6), pp 303-313.

R.Patnaik and D. P. Casasent, 2005 "MINACE-filter-based facial pose estimation" in Biometric Technology for Human Identification., Proc SPIE, pp 460-467.

H. A. Rowley, S. Baluja, and T.Kanade. 1998 "Neural network-based face detection" IEEE PAMI, 20(1):23–38.

Robbins, B., Owens, R. 1997 "2D feature detection via local energy" Image and Vision Computing 15,pp353-368.

R. Schapire and Y. Singer, 1999 "Improved boosting algorithms using confidence-related predictions". Machine Learning, 37(3), pp.297-336.

T. Sim, S. Baker, and M. Bsat,2002 "The CMU Pose, Illumination and Expression (PIE) database," Proc. Fifth IEEE FG, pp. 46-51.

Gründig M. and Hellwich,O., 2004, "3D Head Pose Estimation with Symmetry Based Illumination Model in Low Resolution Video", DAGM, LNCS, pp. 45-53.

C. Yuan and D. P. Casasent,2005 "Face recognition and verification with pose and illumination variations and imposer rejection," in Biometric Technology for Human Identification., Proc SPIE.

S. Zhao and Y. Gao, 2006 "Automated Face Pose Estimation Using Elastic Energy Models", The 18th ICPR, pp.618-621, Vol. 4.